

# The need of appropriate brain SPECT templates for SPM comparisons

S. MORBELLI<sup>1</sup>, G. RODRIGUEZ<sup>2</sup>, A. MIGNONE<sup>3</sup>, V. ALTRINETTI<sup>1</sup>, A. BRUGNOLO<sup>2</sup>,  
A. PICCARDO<sup>1</sup>, A. PUPI<sup>4</sup>, P. M. KOULIBALY<sup>5</sup>, F. NOBILI<sup>2</sup>

**Aim.** Statistical parametric mapping (SPM) is used worldwide to compare brain perfusion single photon emission computed tomography (SPECT) data. The default template within the SPM package used for SPECT image normalization includes images of a group of healthy subjects studied with [<sup>99m</sup>Tc]HMPAO. Since [<sup>99m</sup>Tc]HMPAO and [<sup>99m</sup>Tc]ECD have shown to distribute differently in SPECT studies, we formulated the hypothesis that comparing set of [<sup>99m</sup>Tc]ECD data normalized by means of a [<sup>99m</sup>Tc]HMPAO template may lead to incorrect results.

**Methods.** A customized [<sup>99m</sup>Tc]ECD template was built with SPECT and magnetic resonance imaging (MRI) images of 22 neurologically healthy women. Then, two sets of subjects, *i.e.* a group of patients with very early Alzheimer's disease (eAD) and a matched control group, studied by means of [<sup>99m</sup>Tc]ECD SPECT, were chosen for comparisons. The same statistical approach (t-test between eAD patients and controls and correlation analysis between brain SPECT and a cognitive score) was applied twice, *i.e.* after normalization with either the default [<sup>99m</sup>Tc]HMPAO template or the customized [<sup>99m</sup>Tc]ECD template.

**Results.** In the comparison between eAD and controls, a cluster of difference in the posterior cingulate gyrus of both hemispheres was only highlighted when using the customized [<sup>99m</sup>Tc]ECD template, but was missed when using the default [<sup>99m</sup>Tc]HMPAO template. In the correlation between brain perfusion and a cognitive score, the significant cluster was more significant and far more extended, also including the right superior temporal gyrus, using the customized [<sup>99m</sup>Tc]ECD template than using the default [<sup>99m</sup>Tc]HMPAO template.

**Funding.**—This research project was supported in part by Bristol-Myers Squibb.

Address reprint requests to: S. Morbelli, MD, Nuclear Medicine Unit (DIMI), Viale Benedetto XV 6, 16132 Genoa, Italy.  
E-mail: s.morbe@libero.it

<sup>1</sup>Nuclear Medicine Unit (DIMI), S. Martino University Hospital, Genoa, Italy

<sup>2</sup>Clinical Neurophysiology Unit (DiSEM, DiTeC) S. Martino University Hospital, Genoa, Italy

<sup>3</sup>Nuclear Medicine Unit, Ospedali Riuniti, Bergamo, Italy

<sup>4</sup>Nuclear Medicine Unit (DFP) University of Florence, Florence, Italy

<sup>5</sup>Nuclear Medicine Department, Antoine Lacassagne Center TIRO CEA-University of Nice-Sophia Antipolis, Nice, France

**Conclusion.** These data suggest the need of customized, radiopharmaceutical-matched SPECT templates to be used within the SPM package. The present customized [<sup>99m</sup>Tc]ECD template is now freely available on the web.

**KEY WORDS:** Brain mapping - Tomography, emission-computed, single-photon - Radiopharmaceuticals.

Statistical parametric mapping (SPM)<sup>1</sup> is a worldwide used tool for voxel-based analysis and statistical comparison of functional magnetic resonance imaging (fMRI), positron emission tomography (PET) and single photon emission computed tomography (SPECT) brain studies. As for other image analysis tools, spatial normalization is a crucial preprocessing step in SPM image analysis, because it warps brain volumes acquired from different individuals to fit in a neuroanatomical reference space.<sup>2</sup> It would be advisable that modalities of image acquisition between subjects under investigation and subjects used to build a template for further statistical analysis were as similar as possible, to obtain more reliable results.

This issue has recently been highlighted by Gispert *et al.*,<sup>3</sup> who showed the significant influence of using

the standard SPM PET template in inappropriate conditions on SPM results. In their example, they showed the inadequacy of the [ $^{15}\text{O}$ ]H $_2$ O SPM PET template in a group of schizophrenic patients undergoing [ $^{18}\text{F}$ FDG]PET.

In most nuclear medicine centers, as far as SPECT data are concerned, both [ $^{99\text{m}}\text{Tc}$ ]HMPAO and [ $^{99\text{m}}\text{Tc}$ ]ECD are used to evaluate cerebral blood flow distribution. The two tracers are known to distribute very differently both in the healthy condition<sup>4, 5</sup> and in several diseases, including subacute non cortical stroke,<sup>6</sup> post-stroke reperfusion,<sup>7</sup> herpes simplex encephalitis,<sup>8</sup> temporal lobe epilepsy,<sup>9</sup> brain inflammatory disease,<sup>10</sup> and Alzheimer's disease (AD) patients.<sup>11, 12</sup> When the two compounds were compared to each other, authors found a relatively higher uptake of either of the two tracers in different brain regions. In fact, [ $^{99\text{m}}\text{Tc}$ ]HMPAO uptake is generally reported to be higher than [ $^{99\text{m}}\text{Tc}$ ]ECD uptake in the basal ganglia, cerebellum, thalami and mesial temporal structures whereas [ $^{99\text{m}}\text{Tc}$ ]ECD uptake has been found to be higher than [ $^{99\text{m}}\text{Tc}$ ]HMPAO uptake in mesial occipital cortex, including the lingual gyrus, the cuneus and precuneus, the superior parietal and frontal cortex.<sup>4, 5, 12-15</sup>

However, SPM99, SPM2 and SPM5 software packages<sup>16</sup> contain just a [ $^{99\text{m}}\text{Tc}$ ]HMPAO SPECT normalization template. The absence of a corresponding [ $^{99\text{m}}\text{Tc}$ ]ECD template in SPM packages forces researchers to build, whenever possible, a customized [ $^{99\text{m}}\text{Tc}$ ]ECD template in the case they analyze [ $^{99\text{m}}\text{Tc}$ ]ECD SPECT scans. This procedure has increasingly been followed,<sup>17-20</sup> whereas the inappropriate SPM [ $^{99\text{m}}\text{Tc}$ ]HMPAO 'default' template has still been used in other studies.<sup>21-26</sup> This may have lead to incorrect results, but these inconsistencies have never been specifically investigated.

In this study, we wanted to estimate the influence of using either a [ $^{99\text{m}}\text{Tc}$ ]HMPAO or a [ $^{99\text{m}}\text{Tc}$ ]ECD SPECT template on the results of statistical comparison (SPM99) between [ $^{99\text{m}}\text{Tc}$ ]ECD SPECT of patients with very early AD (eAD) and age-matched healthy controls, one of the commonest comparisons in clinical research work. To this purpose, the same statistical comparisons between eAD patients and controls were performed twice, *i.e.* after normalizing images alternatively either on the default SPM99 [ $^{99\text{m}}\text{Tc}$ ]HMPAO SPECT template or on an original, customized [ $^{99\text{m}}\text{Tc}$ ]ECD SPECT template, that is now freely available on the web.<sup>27</sup>

## Materials and methods

### *Subjects studied to build the original [ $^{99\text{m}}\text{Tc}$ ]ECD template*

A similar procedure as that used to build the [ $^{99\text{m}}\text{Tc}$ ]HMPAO SPM99 template (Figure 1A) was followed. Twenty-two young women outpatients (aged from 18 to 45, mean age 26.11±8.11 years), who had undergone both MRI and [ $^{99\text{m}}\text{Tc}$ ]ECD SPECT examinations in the frame of suspected brain involvement during a systemic illness, were selected. A group of young women was chosen to match as much as possible the features of subjects included in the default [ $^{99\text{m}}\text{Tc}$ ]HMPAO SPM99 template (22 young women). In that case, both examinations were normal, the patient was carefully evaluated by means of a neurological interview and examination. If even these two checks were normal, then the patient was judged to be free of brain involvement, in agreement with the referring clinician at the end of the diagnostic procedure.

### *Single photon emission computed tomography injection, acquisition and reconstruction protocols.*

The subjects were injected *via* a preinserted vein cannula (thus being unaware of injection), while lying on a bed, in a dimly lit room, with eyes closed and ears unplugged, after a 10-min rest. The patients remained there for at least 10 min after injection of about 1 000 MBq of [ $^{99\text{m}}\text{Tc}$ ]ECD (Neurolite, BMS, USA), according to the guidelines of the European Society of Nuclear Medicine.<sup>28</sup>

Image acquisition started between 45 and 90 min after the injection. Scans were acquired by a 2-head  $\gamma$ -camera (Millennium VG, GE, USA), equipped with parallel-hole, low-energy, high-resolution collimators. A step-and-shoot acquisition protocol acquired images through 120 projections, with a radius of rotation of  $\geq 15$  cm. Total counts were between 8 and 10 millions. SPECT images were three-dimensionally reconstructed by the ordered-subset expectation-maximization (OSEM) algorithm with 10 subsets and 8 iterations, followed by Gaussian postfiltering (full width-half maximum  $\approx$  FWHM: 8 mm). The pixel size of reconstructed images is 2.33 mm. Compensation for attenuation has already been performed at the reconstruction stage by the iterative algorithm itself. In this case, the attenuation contour was automatically given by the skull contour and the related anatomical shapes were carefully taken into account.

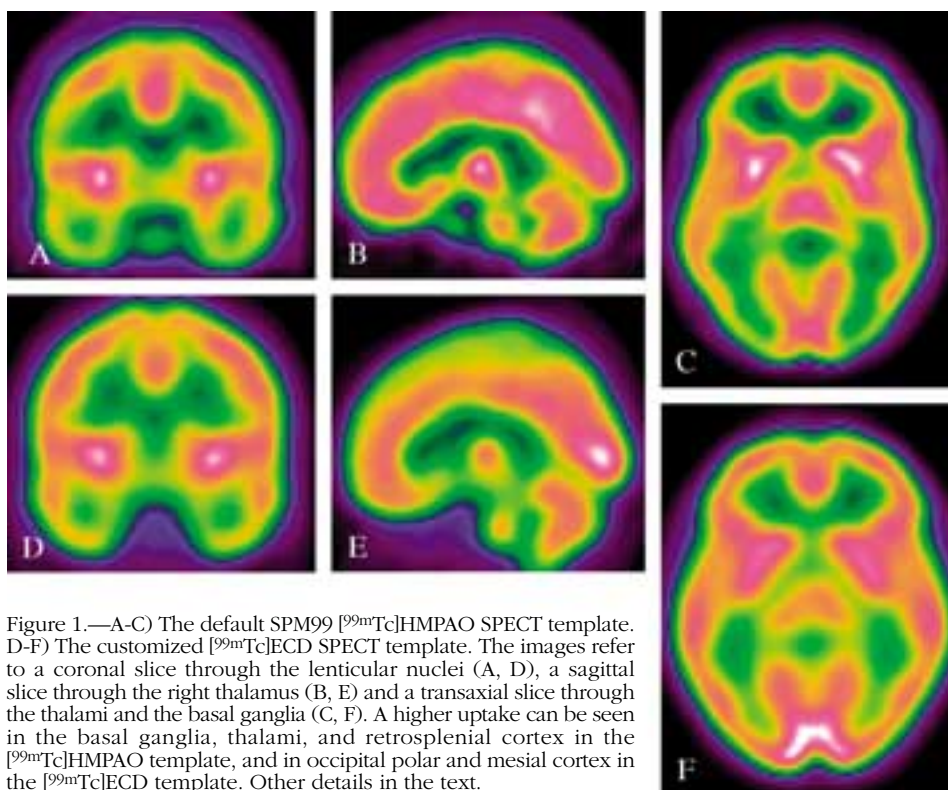


Figure 1.—A-C) The default SPM99 [ $^{99m}\text{Tc}$ ]HMPAO SPECT template. D-F) The customized [ $^{99m}\text{Tc}$ ]ECD SPECT template. The images refer to a coronal slice through the lenticular nuclei (A, D), a sagittal slice through the right thalamus (B, E) and a transaxial slice through the thalami and the basal ganglia (C, F). A higher uptake can be seen in the basal ganglia, thalami, and retrosplenial cortex in the [ $^{99m}\text{Tc}$ ]HMPAO template, and in occipital polar and mesial cortex in the [ $^{99m}\text{Tc}$ ]ECD template. Other details in the text.

### Magnetic resonance imaging acquisition

MRI volumes were obtained using a 1.5-T superconductive equipment (Gyrosan Intera, Philips Medical Systems, Best, The Netherlands) to acquire a T1-FFE sequence with the following parameters: TRs, 20 ms; Tes, 5 ms; FOVs, 250 mm; matrix, 256\*256; 128 sagittal slices (1.6 mm thick); voxel size, 0.98x0.98x1.6.

### Template editing: spatial image normalization and template construction

SPECT normalization was applied using the method previously described by Meyer *et al.*<sup>29</sup> MRI was coregistered (6 parameter, rigid body transformation) to the [ $^{99m}\text{Tc}$ ]ECD SPECT image using a mutual information algorithm included in the SPM99 package. The coregistered MRI was then spatially normalized to the T1-MRI template of SPM99 and the resulting deformation field was applied to SPECT scans (thus, fully MRI-based normalization was performed without the use of any SPECT template). A mean image was cre-

ated from the 22 normalized [ $^{99m}\text{Tc}$ ]ECD SPECT scans and the template was obtained after applying a smoothing isotropic Gaussian filter (FWHM: 8x8x8 mm) (Figure 1B), similarly as for other SPM SPECT and PET templates.<sup>3, 17, 30</sup>

### Patient groups: patients with early Alzheimer's disease and age-matched controls

#### EARLY ALZHEIMER'S DISEASE PATIENTS

Fifteen consecutive AD patients (4 males, 11 females; mean age: 72.2±7.2 years) (*i.e.* with a Mini-Mental State Examination (MMSE) score >20 on first neuropsychological evaluation)<sup>31</sup> were selected from the database of the Dementia Unit of our University Hospital, during a 6-month period. The MMSE score ranged from 22 to 29 (mean: 25.9±2.1), thus qualifying a group of very eAD patients. A diagnosis of probable AD was made according to the definition of the NINCDS-ADRDA Work Group.<sup>32</sup> All the patients underwent a complete diagnostic work-up according to

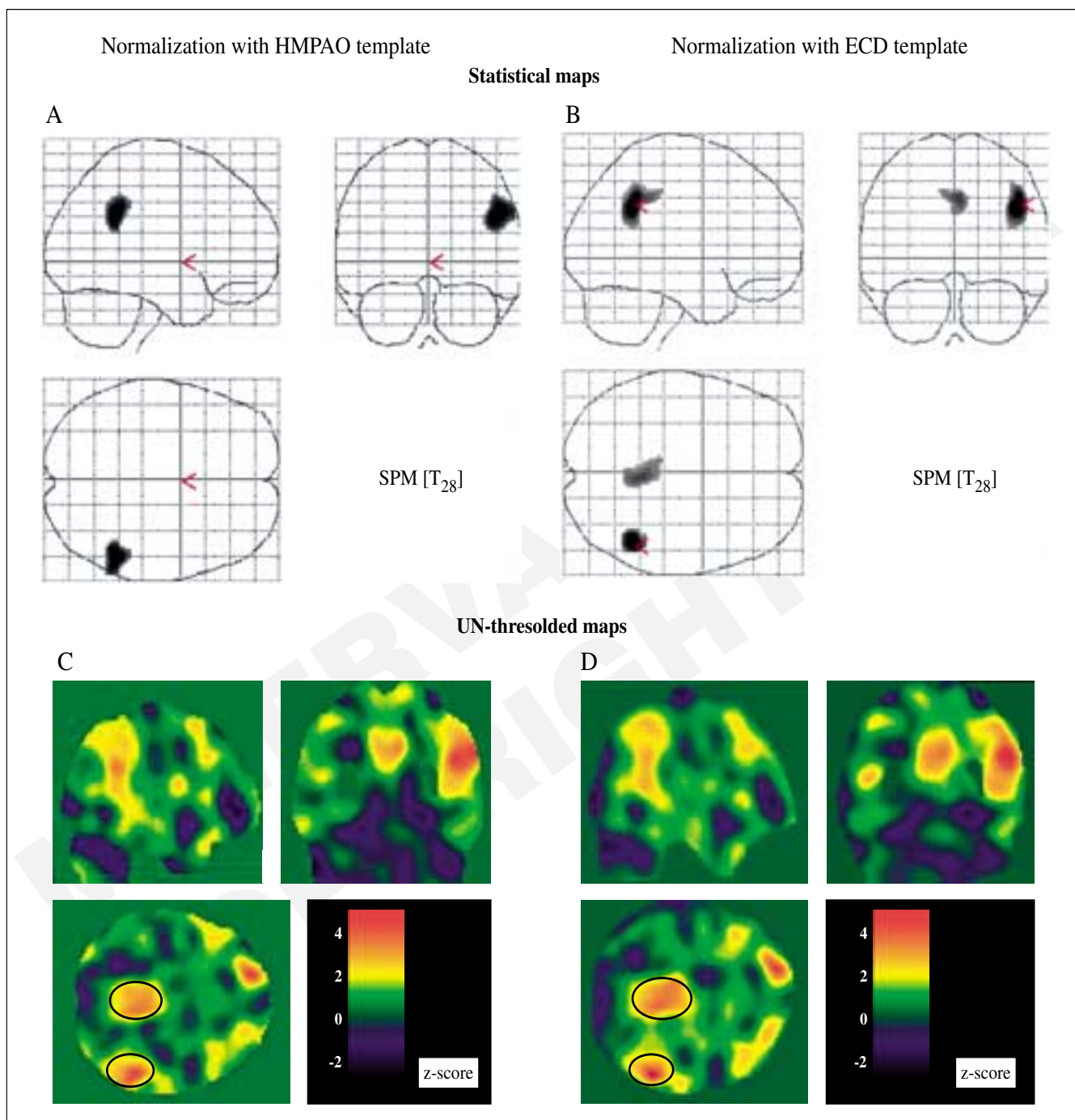


Figure 2.—Results of statistical parametric mapping (SPM) comparison (glass brain) between 15 patients with early AD and 15 aged-matched healthy controls using the two different SPECT templates for normalization (height threshold  $P=0.001$ ). A) Default SPM99  $[^{99m}\text{Tc}]$ HMPAO template; B) customized  $[^{99m}\text{Tc}]$ ECD template. Regions of significant differences between the two groups extend to the posterior cingulate gyrus of both hemispheres with the customized  $[^{99m}\text{Tc}]$ ECD template (B). C, D) Unthresholded maps of the same SPM comparison as above, shown at the level where statistical significance was reached. Elliptical regions of interest are drawn in the transaxial section over the areas reaching the statistical significance. Some difference can be appreciated by visual analysis of these maps as well.

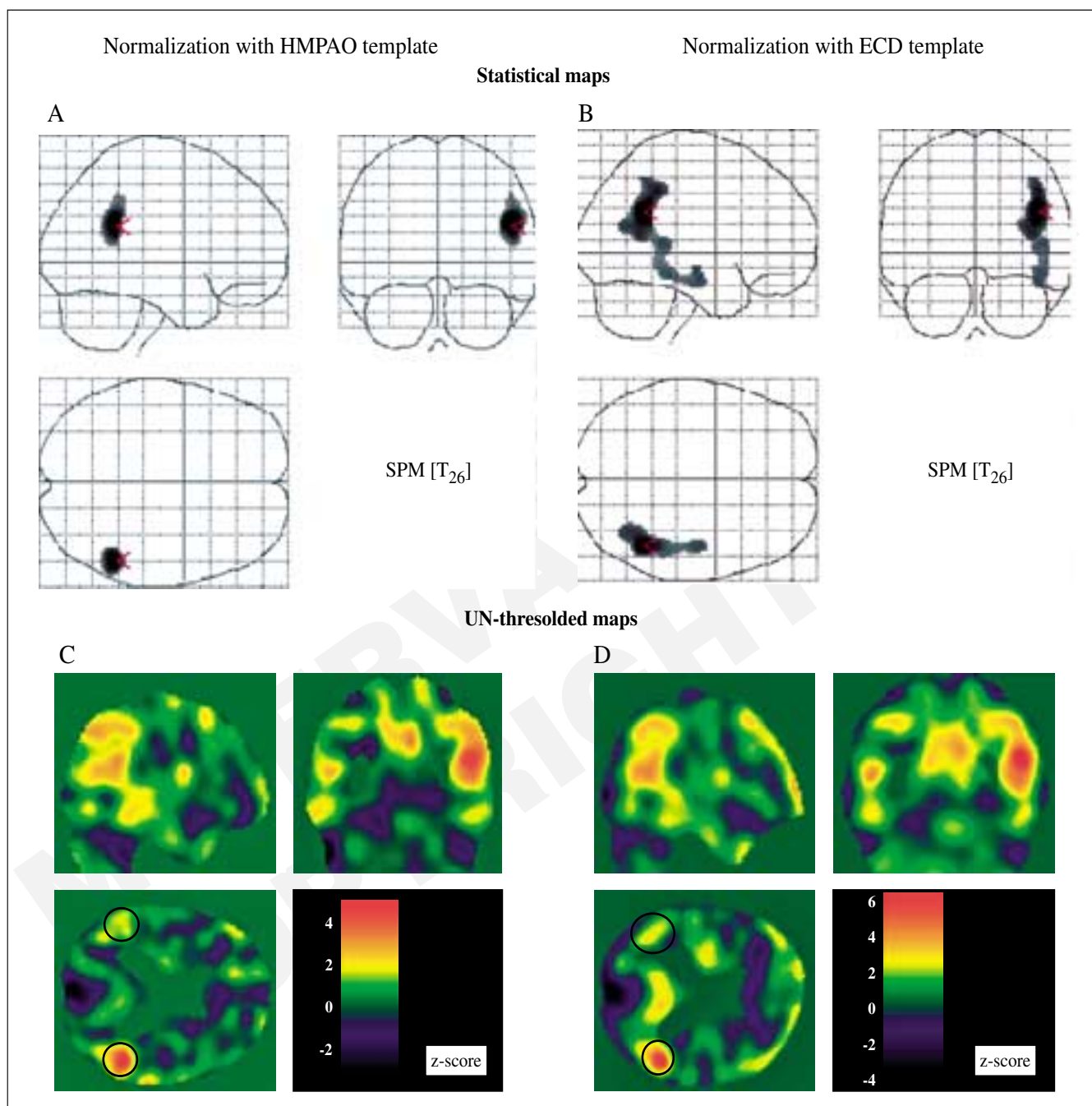


Figure 3.—Results of statistical parametric mapping (SPM) correlation (glass brain) between the MMSE score and brain perfusion in the whole group of 30 subjects (15 healthy controls and 15 AD patients) using the two different SPECT templates for normalization (height threshold  $P=0.001$ ). A) Default SPM99 [ $^{99m}\text{Tc}$ ]HMPAO template; B) customized [ $^{99m}\text{Tc}$ ]ECD template. Correlation is much more extended to the right temporo-parietal cortex with the customized [ $^{99m}\text{Tc}$ ]ECD template (B) than with the default [ $^{99m}\text{Tc}$ ]HMPAO template (A). C, D) Unthresholded maps of the same SPM correlation as above, shown at the level where statistical significance was reached. Elliptical regions of interest are drawn in the transaxial section over the right parietal area reaching the statistical significance and then mirrored to the left one. Note that the z-score scale reaches the value of 6 with the [ $^{99m}\text{Tc}$ ]ECD template and just of 4 with the [ $^{99m}\text{Tc}$ ]HMPAO one. Some difference can be appreciated by visual analysis of these maps as well.

current standards, which include general and neurological examinations, a standardized neuropsychological assessment, a basal MRI (or computed tomography if MRI was inapplicable) and other routine blood and urine screening investigations to rule out secondary dementias. The presence of previous or present major psychiatric disorders, serious neurological diseases, severe and uncontrolled arterial hypertension, diabetes mellitus, renal, hepatic or respiratory failure, anemia (Hb level: <10 mg/dL) or malignancies were exclusion criteria. In conformity with the diagnosis of AD, all patients scored <4 on the Hachinski ischemic scale. Lewy-body dementia, frontotemporal dementia and vascular dementia were excluded in all patients on the basis of current clinical criteria.<sup>33-35</sup> The presence of behavioral and psychological disturbances was assessed by a structured interview to the principal caregiver by means of the neuropsychiatric inventory. All the patients performed [<sup>99m</sup>Tc]ECD SPECT as routine part of diagnostic procedure for early dementia. They were at their first diagnostic evaluation for cognitive complaints, thus none of them were under treatment with acetylcholinesterase inhibitors, nor with other neuropsychotropic drugs. The patients (or their relatives) were informed about the finalities of the study and gave their informed consent.

#### CONTROLS

About 50 subjects older than 50 years were contacted during University courses reserved to elderly people. A prerequisite to be enrolled in the study was to not complain any cognitive disturbance. All subjects were informed about the finality of the study and gave their consent to participate. Forty subjects accepted to participate and underwent brain [<sup>99m</sup>Tc]ECD SPECT examination. All subjects were carefully screened by general medical history and clinical examination. Complete blood count, serum glucose, creatinine and total cholesterol, blood urea nitrogen, and urinalysis were performed and had to be normal for them to be enrolled in the control group. Previous or present neurological, psychiatric, metabolic or cardiovascular disorders, current medication of any kind were the other exclusion criteria. A complete neuropsychological battery, including standard tests for verbal and spatial memory, attention, verbal fluency, executive functions, abstract reasoning and constructional praxis, was administered. Only subjects

with a normal score in all the above tests were considered. Among the control subjects matching these requisites, 15 were selected in the same age range of patients (7 males, 8 females; mean age: 70.7±5.7 years) and formed the control group (MMSE score range: 27-30; mean: 29.3±1.1).

Technetium-99m-ECD SPECT scan was performed with the same modalities and in the same period both in patients and controls as well as in the 22 young women acquired for template editing.

#### Statistical analysis

The SPECT of each eAD patient and control subject was normalized twice. First, using the default SPM99 [<sup>99m</sup>Tc]HMPAO SPECT template. Second, using the original, customized [<sup>99m</sup>Tc]ECD SPECT template. In both cases, deformation was applied by smoothing images with an isotropic Gaussian kernel of FWHM of 12 mm.

SPM99 co-registers the individual SPECT with the 152 brains average of the Montreal Neurological Institute. Since this template does not completely match the Talairach brain, a correction of the SPM{t} coordinates is needed. This was achieved using the subroutine implemented by Brett,<sup>36</sup> which gives the correspondence between SPM and the Talairach atlas coordinates.

The grey matter threshold was set at 0.5, as recommended when examining patients with likely focal hypoperfusion.<sup>37, 38</sup> Normalization of global CBF to 50 was performed with proportional scaling. The resulting set of values for comparison constituted a statistical parametric map of the statistic SPM{t}. Then, the SPM{t} maps were transformed to the unit of normal distribution (SPM{z}) and reached a threshold at  $P=0.001$ . Because of the lack of any topographic a priori hypothesis, the significance of identified regions was assessed using P values, corrected for multiple comparisons ( $P=0.05$  was the first statistical significance to be accepted at the cluster level). Only those significant clusters with more than 100 voxels were considered.

Two comparisons were assessed: 1) comparison (two sample t-test) between eAD patients and controls; 2) correlation (single subject: covariates only) between the MMSE score and brain perfusion in the whole of 30 subjects, including patients and controls.

These two analysis were performed twice, by alternatively using either images normalized with the

TABLE I.—Numerical results of SPM-SPECT comparison (controls-AD) for images normalized using either the default SPM99 [<sup>99m</sup>Tc]HMPAO template or the customized [<sup>99m</sup>Tc]ECD template (height threshold P=0.001).

Analysis	Cluster level			Voxel level			
	Cluster extent	Corrected P value	Cortical region	Z score of maximum	Talairach coordinates	Cortical region	BA
[ <sup>99m</sup> Tc]HMPAO	460	0.011	R-parietal	4.32	48, -45, 30	Supramarginal gyrus	40
[ <sup>99m</sup> Tc]ECD	456	0.011	R-parietal	4.49	48, -47, 36	Inferior parietal lobule	31
	304	0.044	R-parietal	3.75	2, -39, 39	Posterior cingulate gyrus	31
			L-parietal	3.43	-4, -33, 40	Posterior cingulate gyrus	40

A value of P=0.05, corrected for multiple comparison at cluster level, was accepted as statistically significant. In the 'Cluster level' section on left, the number of voxels, the corrected P value of significance and the cortical region, where the cluster is found, are all reported for each significant cluster of correlation. In the 'Voxel level' section, all the coordinates of the correlation sites (with the Z score of the maximum correlation), the corresponding cortical region and BA are reported for each significant cluster. L, left; R, right; BA, Brodmann's area.

TABLE II.—Numerical results of the SPECT-MMSE score correlation for images normalized using either the default SPM99 [<sup>99m</sup>Tc]HMPAO template or the customized [<sup>99m</sup>Tc]ECD template (height threshold P=0.001).

Analysis	Cluster level			Voxel level			
	Cluster extent	Corrected P value	Cortical region	Z score of maximum	Talairach coordinates	Cortical region	BA
[ <sup>99m</sup> Tc]HMPAO	484	0.008	R-parietal	4.4	50, -45, 24	Inferior parietal lobule	40
[ <sup>99m</sup> Tc]ECD	1307	0.000	R-temporal	4.98	44, -49, 28	Superior temporal gyrus	39
			R-parietal	4.04	46, -41, 39	Inferior parietal lobule	40
			R-temporal	3.53	46, -37, 7	Superior temporal gyrus	41

A value of P=0.05, corrected for multiple comparison at cluster level, was accepted as statistically significant. In the 'Cluster level' section on left, the number of voxels, the corrected P value of significance and the cortical region, where the cluster is found, are all reported for each significant cluster of correlation. In the 'Voxel level' section, all the coordinates of the correlation sites (with the Z score of the maximum correlation), the corresponding cortical region and BA are reported for each significant cluster. L, left; R, right; BA, Brodmann's area.

default SPM99 [<sup>99m</sup>Tc]HMPAO template or images normalized with the customized [<sup>99m</sup>Tc]ECD template. Results of comparisons were shown both as thresholded (P=0.001) statistical maps (Figures 2A, B and 3A, B) and as unthresholded maps (Figures 2C, D and 3C, D). Moreover, regions of interest (ROIs) were drawn on trasaxial section over some regions typically affected in eAD and mean z-scores ( $\pm$  standard deviations, SD) were computed in these ROIs.

## Results

Figure 1 shows the two SPECT templates, the default SPM99 [<sup>99m</sup>Tc]HMPAO template (Figure 1A) and the customized [<sup>99m</sup>Tc]ECD template (Figure 1B). Some of the well-known tracer uptake distribution differences between the two radiopharmaceuticals are highlighted by visual analysis. Uptake appears to be higher in the basal ganglia, thalami and pons in the

[<sup>99m</sup>Tc]HMPAO template, whereas it is higher in polar and mesial occipital cortex, posterior parietal cortex, and lateral frontal cortex in the [<sup>99m</sup>Tc]ECD template.

In the comparison between eAD patients and controls, [<sup>99m</sup>Tc]HMPAO template-normalized images showed in eAD patients a significant cluster of reduced uptake in the right parietal supramarginal gyrus (BA 40) (Figure 2A). By using the [<sup>99m</sup>Tc]ECD template-normalized images, a similarly positioned cluster in BA 40 also extended to the right inferior parietal lobule. Moreover, another cluster of significantly reduced uptake was found in the posterior cingulate gyrus of both hemispheres (Figure 2B).

Table I reports in detail the sites of significant SPM clusters for comparison performed with images normalized with either the default [<sup>99m</sup>Tc]HMPAO and Table II the customized [<sup>99m</sup>Tc]ECD template.

As for correlation between the MMSE score and brain perfusion, a significant cluster of positive correlation was found with the default [<sup>99m</sup>Tc]HMPAO

template involving the right inferior parietal lobule (BA 40)(Figure 3A). Again, the correlation with the customized-[<sup>99m</sup>Tc]ECD template yields a different result, because more significant clusters were found not only in the inferior parietal lobule, but also in the right superior temporal gyrus (BA 39 and 41) (Figure 3B) (Tables I and II).

Results of comparison and correlation were also shown as unthresholded maps to highlight the differences even in non significant voxels (Figures 2C, D and 3C, D), as suggested by the approach by Jernigan *et al.*<sup>39</sup> On a transaxial section formed by summing up 4 adjacent slices, elliptical ROIs were drawn on the posterior cingulate and right parietal cortex (eAD *vs* controls; Figures 2C, D) and on the bilateral parietal cortex (correlation between perfusion and MMSE score in the 30 subjects; Figures 3C, D). In the comparison between eAD patients and controls, mean z-scores per voxel were higher with [<sup>99m</sup>Tc]ECD template normalization both in the posterior cingulate ( $2.45 \pm 0.63$  *vs*  $1.92 \pm 0.47$ ) and in the right parietal cortex ( $2.66 \pm 0.25$  *vs*  $2.41 \pm 0.74$ ). In the same direction, mean z-scores per voxel were higher also in the correlation between brain perfusion and MMSE score both in the right ( $2.94 \pm 0.65$  *vs*  $2.23 \pm 0.52$ ) parietal cortex that reached the statistical significance and in the left parietal cortex ( $1.53 \pm 0.7$  *vs*  $1.21 \pm 0.45$ ) not reaching the statistical significance.

## Discussion

This study shows that the results of [<sup>99m</sup>Tc]ECD SPECT SPM comparisons vary depending on the template used to normalize images. The results obtained with the customized [<sup>99m</sup>Tc]ECD template appear to be more meaningful than those obtained with the default [<sup>99m</sup>Tc]HMPAO one.

For instance, the hypoperfusion in bilateral posterior cingulate gyrus, typically reported in early AD,<sup>40, 41</sup> was only highlighted by the use of [<sup>99m</sup>Tc]ECD template, but was missed by the use of [<sup>99m</sup>Tc]HMPAO template. The early involvement of the posterior cingulate was first shown by means of [<sup>18</sup>F]FDG PET<sup>42</sup> and then confirmed by SPECT studies as well.

Moreover, the clusters of correlation between brain perfusion and the MMSE score (a widely used index of global cognitive impairment) achieved with the [<sup>99m</sup>Tc]ECD template normalization extended to involve larger areas of the posterior associative cortex, including the lateral temporal cortex (BA 39 and 41) and the

inferior parietal lobule in the right hemisphere. Both these areas are known to be affected by hypoperfusion in eAD and their involvement contributes to the cognitive failure.<sup>23, 43</sup> Also the analysis of unthresholded maps produced by the SPM99 software showed both visual and ROI z-score differences between the comparisons performed using the two templates. This was highlighted both in ROIs drawn at the level of significant areas and in a ROI drawn where the statistical significance was not reached (the left parietal cortex in the perfusion-MMSE score correlation). This finding further confirms that the results obtained using the two templates in the normalization step are different.

The current model for the interpretation of brain hypometabolism/hypoperfusion findings in eAD is based on the theory of functional disconnection of these posterior temporal-parietal associative regions from the mesial temporal cortex, where pathological changes are found early.<sup>43</sup>

The differences between the default [<sup>99m</sup>Tc]HMPAO SPM template and the present customized [<sup>99m</sup>Tc]ECD one do not concern the radiopharmaceutical only. In fact, in the SPM template, SPECT were acquired with a 3-head camera equipped with LEUHR, fan-beam collimators and images were reconstructed with a filtered back-projection algorithm. On the other hand, in the present customized [<sup>99m</sup>Tc]ECD template, SPECT were acquired with a 2-head camera equipped with LEHR, parallel-hole collimators and images were reconstructed with an OSEM algorithm. The relative weight of these factors cannot be ascertained with the present data, but the crucial point is that the customized template was built exactly with the same image acquisition modalities as for patients under study. A consequent conclusion would be that a specific template should be available at least for each radiopharmaceutical, while the influence of different equipments (number of heads and collimators) and reconstruction algorithms deserve further investigation. Since this is hardly feasible in most nuclear medicine centers, the free availability of the present customized [<sup>99m</sup>Tc]ECD template on the web<sup>27</sup> could help those researchers working with [<sup>99m</sup>Tc]ECD and a two-head camera equipped with parallel-hole collimators, which is probably the most distributed worldwide.

## Conclusions

The present results further confirm that the two radiopharmaceuticals are very different indeed. Even

in a normalization procedure with gross smoothing, such differences survive and can modify the results of the statistical comparisons. This finding, together with the similar demonstration of the mismatch between the [ $^{18}\text{F}$ FDG]PET and the [ $^{15}\text{O}$ ]H $_2$ O-PET SPM templates,<sup>3</sup> suggests an effort to build proper templates for each radiopharmaceutical, with scans acquired and reconstructed with the same modalities as the groups under study, to achieve methodologically sound data. To note that several centers are now applying SPM comparison between single case study and a control group,<sup>44, 45</sup> to confirm or highlight areas of perfusion abnormalities seen during conventional visual reporting. This further stresses the need to have access to proper templates.

## References

- Friston KJ, Holmes AP, Worsley KJ, Poline JP, Frith CD, Frackowiak RSJ. Statistical parametric maps in functional imaging: a general linear approach. *Hum Brain Mapping* 1995;2:189-210.
- Talairach J, Tournoux P. Co-planar stereotaxic atlas of the human brain. New York: Thieme Medical; 1988.
- Gispert JD, Pascau J, Reig S, Martinez-Lazaro R, Molina V, Garcia-Barreno P *et al*. Influence of the normalization template on the outcome of statistical parametric mapping of PET scans. *Neuroimage* 2003;19:601-12.
- Koyama M, Kawashima R, Ito H, Ono S, Sato K, Goto R *et al*. SPECT imaging of normal subjects with technetium-99m-HMPAO and technetium-99m-ECD. *J Nucl Med* 1997;38:587-92.
- Patterson JC, Early TS, Martin A, Walker MZ, Russell JM, Villanueva-Meyer H. SPECT image analysis using statistical parametric mapping: comparison of technetium-99m-HMPAO and technetium-99m-ECD. *J Nucl Med* 1997;38:1721-5.
- Hyun IY, Lee JS, Rha JH, Lee IK, Ha CK, Lee DS. Different uptake of  $^{99\text{m}}\text{Tc}$ -ECD and  $^{99\text{m}}\text{Tc}$ -HMPAO in the same brains: analysis by statistical parametric mapping. *Eur J Nucl Med* 2001;28:191-7.
- Ogasawara K, Ogawa A, Ezura M, Konno H, Suzuki M, Yoshimoto T. Brain single-photon emission CT studies using  $^{99\text{m}}\text{Tc}$ -HMPAO and  $^{99\text{m}}\text{Tc}$ -ECD early after recanalization by local intraarterial thrombolysis in patients with acute embolic middle cerebral artery occlusion. *Am J Neuroradiol* 2001;22:48-53.
- Rieck H, Adelwohrer C, Lungenschmid K, Deisenhammer E. Discordance of technetium-99m-HMPAO and technetium-99m-ECD SPECT in herpes simplex encephalitis. *J Nucl Med* 1998;39:1508-10.
- Lee SK, Lee DS, Yeo JS, Lee JS, Kim YK, Jang MJ *et al*. Superiority of HMPAO ictal SPECT to ECD ictal SPECT in localizing the epileptogenic zone. *Epilepsia* 2002;43:263-9.
- Shuke N, Saito K, Morimoto M, Kubota T, Shibata K, Saito Y *et al*. Brain perfusion SPECT in neuro-Behcet's disease: discordance between Tc-99m-HMPAO and Tc-99m-ECD. *Ann Nucl Med* 1996;10:353-6.
- Koulibaly PM, Nobili F, Migneco O, Vitali P, Robert PH, Girtler N *et al*.  $^{99\text{m}}\text{Tc}$ -HMPAO and  $^{99\text{m}}\text{Tc}$ -ECD perform differently in typically hypoperfused areas in Alzheimer's disease. *Eur J Nucl Med Mol Imaging* 2003;30:1009-13.
- Nobili F, Koulibaly PM, Rodriguez G, Benoit M, Girtler N, Robert PH *et al*. (99m)Tc-HMPAO and (99m)Tc-ECD brain uptake correlates of verbal memory in Alzheimer's disease. *Q J Nucl Med Mol Imaging* 2007; [Epub ahead of print].
- Leveille J, Demonceau G, Walovitch RC. Intrasubject comparison between Technetium-99m-ECD and Technetium-99m-HMPAO in healthy human subjects. *J Nucl Med* 1992;33:480-4.
- Oku N, Matsumoto M, Hashikawa K, Moriwaki H, Ishida M, Seike Y *et al*. Intraindividual differences between technetium-99m-ECD and technetium-99m-HMPAO in the normal medial temporal lobe. *J Nucl Med* 1997;38:1109-11.
- Asenbaum S, Brucke T, Pirker W, Pietrzyk U, Podreka I. Imaging of cerebral blood flow with technetium-99m-HMPAO and technetium-99m-ECD: a comparison. *J Nucl Med* 1998;39:613-8.
- Friston K, Ashburner J, Heather J, Holmes A, Poline JB. Statistical parametric mapping. The Wellcome Department of Cognitive Neurology, University College of London, London. (<http://www.fil.ion.ucl.ac.uk/spm>).
- Kogure D, Matsuda H, Ohnishi T, Asada T, Uno M, Kunihiko T *et al*. Longitudinal evaluation of early Alzheimer's disease using brain perfusion SPECT. *J Nucl Med* 2000;41:1155-62.
- Ohnishi T, Matsuda H, Hashimoto T, Kunihiko T, Nishikawa M, Uema T *et al*. Abnormal regional cerebral blood flow in childhood autism. *Brain* 2000;123:1838-44.
- Caroli A, Testa C, Geroldi C, Nobili F, Guerra UP, Bonetti M *et al*. Brain perfusion correlates of medial temporal lobe atrophy and white matter hyperintensities in mild cognitive impairment. *J Neurol* 2007; [Epub ahead of print].
- Matsuda H, Kitayama N, Ohnishi T, Asada T, Nakano S, Sakamoto S *et al*. Longitudinal evaluation of both morphologic and functional changes in the same individuals with Alzheimer's disease. *J Nucl Med* 2002;43:304-11.
- Migneco O, Benoit M, Koulibaly PM, Dygai I, Bertogliati C, Desvignes P *et al*. Perfusion brain SPECT and statistical parametric mapping analysis indicate that apathy is a cingulate syndrome: a study in Alzheimer's disease and nondemented patients. *Neuroimage* 2001;13:896-902.
- Rolland Y, Payoux P, Lauwers-Cances V, Voisin T, Esquerre JP, Vellas B. A SPECT study of wandering behavior in Alzheimer's disease. *Int J Geriatr Psychiatry* 2005;20:816-20.
- Rodriguez G, Morbelli S, Brugnolo A, Calvini P, Girtler N, Piccardo A *et al*. Global cognitive impairment should be taken into account in SPECT-neuropsychology correlations: the example of verbal memory in very mild Alzheimer's disease. *Eur J Nucl Med Mol Imaging* 2005;32:1186-92.
- Borroni B, Anchisi D, Paghera B, Vicini B, Kerrouche N, Garibotto V *et al*. Combined  $^{99\text{m}}\text{Tc}$ -ECD SPECT and neuropsychological studies in MCI for the assessment of conversion to AD. *Neurobiol Aging* 2006;27:24-31.
- Joo EY, Hong SB, Tae WS, Han SJ, Seo DW, Lee KH *et al*. Effect of lamotrigine on cerebral blood flow in patients with idiopathic generalised epilepsy. *Eur J Nucl Med Mol Imaging* 2006;33:724-9.
- Choi JY, Lee KH, Na DL, Byun HS, Lee SJ, Kim H *et al*. Subcortical aphasia after striatocapsular infarction: quantitative analysis of brain perfusion SPECT using statistical parametric mapping and a statistical probabilistic anatomic map. *J Nucl Med* 2007;48:194-200.
- Available at: <http://www.aimn.it>
- Tatsch K, Asenbaum S, Bartenstein P, Catafau A, Halldin C, Pilowsky LS *et al*. European Association of Nuclear Medicine Procedure Guidelines for Brain Perfusion SPET Using  $^{99\text{m}}\text{Tc}$ -Labelled Radiopharmaceuticals. *Eur J Nucl Med* 2002;29:BP36-BP42.
- Meyer JH, Gunn RN, Myers R, Grasby PM. Assessment of systematic and quantitative review of volumetric magnetic resonance imaging studies. *Neuroimage* 1999;9:545-53.
- Colloby SJ, O'Brien JT, Fenwick JD, Firbank MJ, Burn DJ, McKeith IG *et al*. The application of statistical parametric mapping to  $^{123}\text{I}$ -FP-CIT SPECT in dementia with Lewy bodies, Alzheimer's disease and Parkinson's disease. *Neuroimage* 2004;23:956-66.
- Folstein MF, Folstein SE, McHugh PR. 'Mini Mental State': a practical method for grading the cognitive state of patients for clinician. *J Psychiatr Res* 1975;12:189-98.

32. McKhann G, Drachman D, Folstein M, Katzman R, Price D, Stadlan E. Clinical diagnosis of Alzheimer's disease: report of the NINCDS ADRDA work group under the auspices of the Department of Health and Human Services Task Force on Alzheimer's Disease. *Neurology* 1984;34:939-44.
33. McKeith IG, Dickson DW, Lowe J, Emre M, O'Brien JT, Feldman H *et al*. Diagnosis and management of dementia with Lewy bodies: third report of the DLB Consortium. *Neurology* 2005;65:1863-72.
34. The Lund and Manchester Groups. Clinical and neuropathological criteria for frontotemporal dementia. *J Neurol Neurosurg Psychiatry* 1994;57:416-8.
35. Roman GC, Tatemichi TK, Erkinjuntti T, Cummings JL, Masdeu JC, Garcia JH *et al*. Vascular dementia: diagnostic criteria for research studies. Report of the NINDSAIREN International Workshop. *Neurology* 1993;43:250-60.
36. CBU imaging wiki [homepage on the Internet]. CBU Imaging Website. Copyright MRC Cognition and Brain Sciences Unit 2006. [updated 2007 February 23; cited ?????]. Available at: <http://www.mrc-cbu.cam.ac.uk/Imaging>
37. Desgranges B, Baron JC, de la Sayette V, Petit-Taboué MC, Benali K, Landeau B *et al*. The neural substrates of memory systems impairment in Alzheimer's disease. A PET study of resting brain glucose utilisation. *Brain*. 1998;121:611-31.
38. Stamatakis EA, Glabus MF, Wyper DJ, Barnes A, Wilson JTL. Validation of statistical parametric mapping (SPM) in assessing cerebral lesions: a simulation study. *Neuroimage* 1999;10:397-407.
39. Jernigan TL, Gamst AC, Fennema-Notestine C, Ostergaard AL. More "mapping" in brain mapping: statistical comparison of effects. *Hum Brain Map* 2003;19:90-5.
40. Huang C, Wahlund LO, Svensson L, Winblad B, Julin P. Cingulate cortex hypoperfusion predicts Alzheimer's disease in mild cognitive impairment. *BMC Neurol* 2002;2:9.
41. Bonte FJ, Harris TS, Roney CA, Hynan LS. Differential diagnosis between Alzheimer's and frontotemporal disease by the posterior cingulate sign. *J Nucl Med* 2004;45:771-4.
42. Mosconi L. Brain glucose metabolism in the early and specific diagnosis of Alzheimer's disease. FDG-PET studies in MCI and AD. *Eur J Nucl Med Mol Imaging* 2005;32:486-510.
43. Braak H, Braak E. Staging of Alzheimer's disease-related neurofibrillary changes. *Neurobiol Aging* 1995;16:271-8.
44. Signorini M, Paulesu E, Friston K, Perani D, Colleluori A, Lucignani G *et al*. Rapid assessment of regional cerebral metabolic abnormalities in single subjects with quantitative and nonquantitative [<sup>18</sup>F]FDG PET: A clinical validation of statistical parametric mapping. *Neuroimage* 1999;9:63-80.
45. Asada T, Matsuda H, Morooka T, Nakano S, Kimura M, Uno M. Quantitative single photon emission tomography for the diagnosis of transient global amnesia: adaptation of statistical parametric mapping. *Psychiatry Clin Neurosci* 2000;54:691-4.